

Multispectral fluorescence imaging as a tool to separate healthy and disease related lymphatic anatomies during robot-assisted laparoscopic procedures.

Philippa Meershoek^{1,2†}, Gijs H. KleinJan^{1,2†}, Matthias N. van Oosterom¹, Esther M.K. Wit², Danny M. van Willigen¹, Kevin P. Bauwens³, Erik J. van Gennep⁴, Alexandre M. Mottrie^{3,5}, Henk G. van der Poel², Fijs W.B. van Leeuwen^{1,2*}

1 Interventional Molecular Imaging Laboratory, Department of Radiology, Leiden University Medical Center, Leiden, the Netherlands

2 Department of Urology, Netherlands Cancer Institute-Antoni van Leeuwenhoek Hospital, Amsterdam, the Netherlands

3 Orsi Academy, Melle, Belgium

4 Department of Urology, Leiden University Medical Center, Leiden, the Netherlands

5 Department of Urology, Onze-Lieve-Vrouw Hospital, Aalst, Belgium

† shared first-authorship

* corresponding author

Disclaimer:

KB and AM are affiliated with Orsi Academy. No other potential conflicts of interest relevant to this article exist.

Financial support:

This research was financially supported by an NWO-STW-VIDI grant (STW BGT11272), and a European Research Council grant (2012-306890).

Word count:

2495

Short title:

Dual-color surgical guidance

Corresponding author (contact for full information):

Fijs W.B. van Leeuwen

Interventional Molecular Imaging Laboratory
Department of Radiology
Leiden University Medical Center (LUMC)
Albinusdreef 2, PO Box 9600, postal zone C2-S
2300 RC, Leiden
The Netherlands

tel. +31(0)715266029 or +31(0)610173948

tel. (secretary) +31(0)71 526 4376

fax. +31(0)71 5248256

E-mail. F.W.B.van_Leeuwen@lumc.nl

First authors:

Philippa Meershoek and Gijs H. KleinJan

Interventional Molecular Imaging Laboratory
Department of Radiology
Leiden University Medical Center (LUMC)
Albinusdreef 2, PO Box 9600, postal zone C2-S
2300 RC, Leiden
The Netherlands

tel. +31(0)715262042

tel. (secretary) +31(0)71 526 2052

fax. +31(0)71 5248256

E-mails. P.Meershoek@lumc.nl G.H.Kleinjan@lumc.nl

ABSTRACT

To reduce the invasive nature of extended pelvic lymph node dissections (ePLND) in prostate cancer, we have developed a multicolor fluorescence guidance approach that enables the discrimination between prostate draining lymph nodes (LNs) and lower limb draining LNs.

Methods

In five porcine models multispectral-fluorescence guidance was performed using da Vinci Si- and Xi-robot consoles. They received fluorescein into the lower limb(s) and indocyanine green (ICG)-nanocolloid into the prostate.

Results

Fluorescein was detected in 29 LNs (average of 3.6 LNs/template); ICG-nanocolloid visualized 12 LNs (average of 1.2 LNs/template). Signal intensities appeared equal for both dyes and no visual overlap in the lymphatic drainage patterns was observed. Furthermore, fluorescein supported both the identification of leakage from damaged lymphatic structures and the identification of ureters.

Conclusion

We demonstrated that the different lymphatic flow patterns from the prostate and lower limbs could be intraoperatively distinguished using multispectral-fluorescence imaging approaches.

Keywords:

Image guided surgery, prostate cancer, fluorescence, multiplexing, robotic surgery

INTRODUCTION

The metastatic pattern of prostate cancer to the lymphatic system has resulted in the European Association of Urology guidelines recommending extended pelvic lymph node dissection (ePLND) for intermediate- and high risk prostate cancer patients with an estimated risk of nodal metastases exceeding 5% based on Briganti or Kattan nomogram (1). Unfortunately, ePLND induces surgical damage to the natural lymphatic flow in the pelvis resulting in an increased complication rate (2-4), with lymphoceles (10.3%) and lymphedema (4.1%) being the most common (5,6).

For indications such as breast and penile cancer, minimally invasive sampling of the so-called first tumor draining lymph nodes, i.e. sentinel nodes (SNs), has helped reduce the number of patients requiring a LND by >75% (7-9). However, pelvic SN dissections in intermediate- and high-risk prostate cancer patients is a one-stop-shop procedure that includes ePLND, since surgical re-exploration of the pelvic nodal basins after SN sampling is cumbersome and relying solely on SN sampling would leave tumor bearing non-SN in situ in 27.1% of LN-positive patients (7). This setting creates the demand for technologies that preserve the oncological outcome of an ePLND, but that reduces its impact on healthy lymphatic structures not related to the target organ. When available, such an approach could create a paradigm shift for the surgical treatment of lymphatic disease, changing the focus from “removing nodes that count” to “sparing nodes that are not involved”.

We hypothesized that real-time fluorescence multiplexing could allow us to differentiate the pelvic lymphatic drainage profiles of healthy tissues (lower limb) from those of the primary tumor (prostate), respectively (Fig. 1). For this we used the spectrally differentiated lymphangiographic tracer fluorescein and the SN specific tracer indocyanine green (ICG)-nanocolloid (10). We evaluated this concept during robotic pelvic LND procedures in porcine models to demonstrate that: 1) the ICG-tailored da Vinci fluorescence laparoscopes are also capable of imaging the clinically approved visible dye fluorescein and support multispectral-imaging applications, 2) multicolor- or multispectral-fluorescence imaging supports real-time intraoperative separation of the lower limb- and prostate-related lymphatic anatomies, and 3) imaging of fluorescein helps visualize damage to the lymphatic network and highlights ureters.

MATERIALS AND METHODS

Camera Setup

The study was performed using two generations of clinical grade surgical-robotic systems (da Vinci Si and Xi; Intuitive Surgical Inc.) and their integrated Firefly fluorescence laparoscopes. In the surgical console, with both systems processed fluorescent signals were displayed as artificially colored bright green over a grayscale background image. Only with the older Si system it was also possible to display the raw, unprocessed video signal.

Preclinical Evaluation Setup

The multispectral-fluorescence imaging setup was evaluated in five male porcine models during surgical training (Orsi-Academy). The studies were allowed by the Ethical Committee for animal experiments of Gent University (EC2015-152).

To identify the lymphatic drainage of the lower limbs, 5mL fluorescein was administered (100 mg/mL solution) in 2.5mL subcutaneously and 2.5mL intramuscular into the right hind leg (pigs one and two) or deposits of 1.25mL in both hind legs (pigs three, four and five)(Fig. 1). Following fluorescein administration (after 70 – 150 minutes), though preceding ICG-nanocolloid injection, the pelvic area was evaluated for fluorescein positive LNs using both white light and fluorescence imaging.

To allow for lymphatic mapping of the prostate ICG-nanocolloid was used. This tracer was prepared similarly as was previously described for the radiolabeled analogue (11), resulting in a 2 mL solution with 0.125 mg/mL ICG and was injected intra-operatively using a 2mL syringe attached to an injection needle using flexible tubing. After insertion, the surgeon then placed two to four tracer deposits into the prostate using the robotic arms (Fig. 1). Following ICG-nanocolloid injection, the pelvic area was examined for both tracers during a 15-30 minute period.

RESULTS

Overall Performance Fluorescein Imaging versus ICG Imaging

In the processed images of the Si and Xi set-ups, both the fluorescent signals of fluorescein and ICG-nanocolloid were displayed with a green coloration (Fig. 2). Differentiation between the two fluorescent signals required use of the white light images to define the location of fluorescein and/or sequential administration and imaging of fluorescein and ICG-nanocolloid. The ability to use the unprocessed images of the Si system, which displays the two fluorescent signals as yellow/green or red/pink coloration, respectively, made differentiation between the signals much more straight forward (Fig. 3).

In Vivo Experiments

During surgery (~2h post injection) fluorescein was detectable in leg-draining LNs (3.6 LNs/template) in the white light images but was more easily defined in the fluorescence setting (Figs. 2 and 3). Fluorescein leakage provided a valuable indicator for surgical damage of fluorescein containing lymphatics (Fig. 4). Further, the biological (renal) clearance of fluorescein supported fluorescence-based visualization of the ureters (Fig. 4)(12). When using the fluorescence setting, prostate draining SNs (1.2 SNs/template) and lymphatic ducts became visible within minutes after administration of ICG-nanocolloid. Similar to the clinically used ICG-^{99m}Tc-nanocolloid (10), ICG-nanocolloid did not contaminate the surgical field when lymphatic resections were performed.

A clear dividing line was observed between the lymphatic drainage pattern of the prostate and lower limbs; no signal overlap was observed between the lymphatic drainage profiles of the two dyes imaged (Table 1). Differentiation could even occur in the same template (Fig. 3).

DISCUSSION

To our knowledge, this study is the first to demonstrate the fluorescein and multispectral-imaging capabilities of the da Vinci Si and Xi robots. With this technology, a successful distinction was made between ICG-nanocolloid and fluorescein positive lymphatics. Despite the theoretical advantages of near-

infrared dyes, both dyes could be clearly visualized *in vivo* (Figs. 2 and 3). With this multicolor guidance concept, healthy lymphatic structures could potentially be spared, converting to a reduction of lymphedema of the lower limb. The fact that commercially available and clinically approved robotic systems allow such a multispectral-imaging approach, facilitates the translational aspect of these studies. Further clinical follow-up studies are needed to validate the impact of the proposed imaging concept on the outcome in clinical trials.

Next to visualizing the lymphatic drainage patterns of the lower limbs, fluorescein imaging also supported the identification of damage to these same lymphatics; a similar contamination was reported in studies where “free” ICG was used (13). In line with literature, the ureters could also be visualized during surgery using fluorescein (Fig. 4)(14).

Combined with previous reports (10,15,16), the favorable *in vivo* visualization of fluorescein using the da Vinci robotic platform again debates the monopoly of near-infrared approaches in the field of fluorescence-guided surgery.

CONCLUSION

The multispectral-imaging properties of the fluorescence laparoscopes of the da Vinci robotic platform helped realize an intraoperative differentiation between prostate-related (ICG-nanocolloid) and lower limbs-related lymphatic structures, lymphatic damage, and ureters (fluorescein). With that a technology has become available that supports a further improvement of the balance between cure and surgically induced side-effects.

ACKNOWLEDGMENTS

We would like to thank Nikolaos Grivas from the Netherlands Cancer Institute-Antoni van Leeuwenhoek Hospital for his support and assistance.

REFERENCES

1. Briganti A, Larcher A, Abdollah F, et al. Updated nomogram predicting lymph node invasion in patients with prostate cancer undergoing extended pelvic lymph node dissection: the essential importance of percentage of positive cores. *Eur Urol*. 2012;61:480-487.
2. Geppert B, Persson J. Robotic infrarenal paraaortic and pelvic nodal staging for endometrial cancer: feasibility and lymphatic complications. *Acta Obstet Gynecol Scand*. 2015;94:1074-1081.
3. Todo Y, Yamazaki H, Takeshita S, et al. Close relationship between removal of circumflex iliac nodes to distal external iliac nodes and postoperative lower-extremity lymphedema in uterine corpus malignant tumors. *Gynecol Oncol*. 2015;139:160-164.
4. Yamazaki H, Todo Y, Takeshita S, et al. Relationship between removal of circumflex iliac nodes distal to the external iliac nodes and postoperative lower-extremity lymphedema in uterine cervical cancer. *Gynecol Oncol*. 2015;139:295-299.
5. Briganti A, Chun FK, Salonia A, et al. Complications and other surgical outcomes associated with extended pelvic lymphadenectomy in men with localized prostate cancer. *Eur Urol*. 2006;50:1006-1013.
6. Clark T, Parekh DJ, Cookson MS, et al. Randomized prospective evaluation of extended versus limited lymph node dissection in patients with clinically localized prostate cancer. *J Urol*. 2003;169:145-147; discussion 147-148.
7. Wit EMK, Acar C, Grivas N, et al. Sentinel node procedure in prostate cancer: a systematic review to assess diagnostic accuracy. *Eur Urol*. 2017;71:596-605.
8. Wawroschek F, Vogt H, Wengenmair H, et al. Prostate lymphoscintigraphy and radio-guided surgery for sentinel lymph node identification in prostate cancer. Technique and results of the first 350 cases. *Urol Int*. 2003;70:303-310.
9. Holl G, Dorn R, Wengenmair H, Weckermann D, Sciuk J. Validation of sentinel lymph node dissection in prostate cancer: experience in more than 2,000 patients. *Eur J Nucl Med Mol Imaging*. 2009;36:1377-1382.
10. van den Berg NS, Buckle T, KleinJan GH, van der Poel HG, van Leeuwen FWB. Multispectral fluorescence imaging during robot-assisted laparoscopic sentinel node biopsy: a first step towards a fluorescence-based anatomic roadmap. *Eur Urol*. 2017;72:110-117.
11. Brouwer OR, Buckle T, Vermeeren L, et al. Comparing the hybrid fluorescent-radioactive tracer indocyanine green-99mTc-nanocolloid with 99mTc-nanocolloid

for sentinel node identification: a validation study using lymphoscintigraphy and SPECT/CT. *J Nucl Med.* 2012;53:1034-1040.

12. van Leeuwen FW, Hardwick JC, van Erkel AR. Luminescence-based imaging approaches in the field of interventional molecular imaging. *Radiology.* 2015;276:12-29.

13. Nguyen DP, Huber PM, Metzger TA, Genitsch V, Schudel HH, Thalmann GN. A specific mapping study using fluorescence sentinel lymph node detection in patients with intermediate- and high-risk prostate cancer undergoing extended pelvic lymph node dissection. *Eur Urol.* 2016;70:734-737.

14. Udshmadshuridze NS, Asikuri TO. [Intra-operative imaging of the ureter with sodium fluorescein]. *Z Urol Nephrol.* 1988;81:635-639.

15. van Willigen DM, van den Berg NS, Buckle T, et al. Multispectral fluorescence guided surgery; a feasibility study in a phantom using a clinical-grade laparoscopic camera system. *Am J Nucl Med Mol Imaging.* 2017;7:138-147.

16. Buckle T, van Willigen DM, Spa SJ, et al. Tracers for fluorescence-guided surgery: how elongation of the polymethine chain in cyanine dyes alters the pharmacokinetics of a (bimodal) c[RGDyK] tracer. *J Nucl Med.* 2018;E-pub ahead of print.

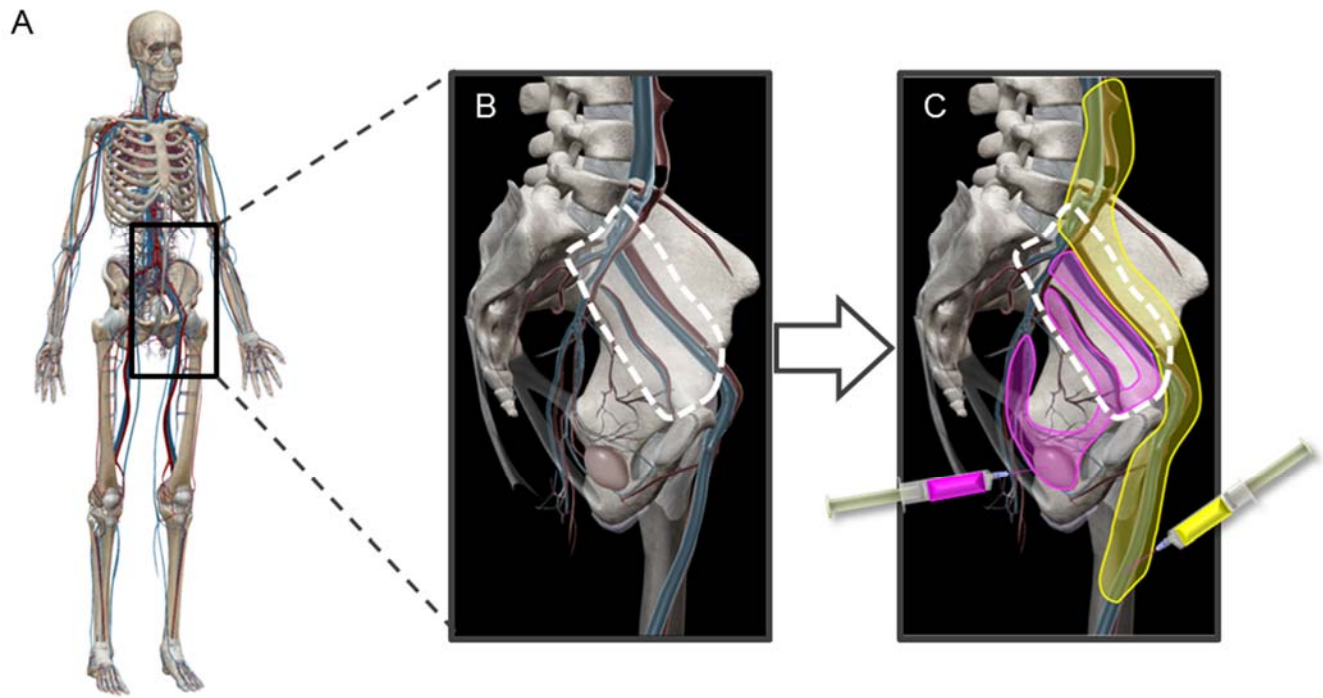


FIGURE 1. Schematic illustration of relevant anatomical structures within the patient (A). (B) All lymphatic structures within the template (white dotted line) get resected during a lymph node resection. (C) Schematic illustration of lower limb (yellow; fluorescein) and prostate (pink; sentinel nodes; ICG-nanocolloid) drainage patterns that pass through the template. The schematic anatomical images were generated with Visible Body software (Argosy Publishing Inc.).

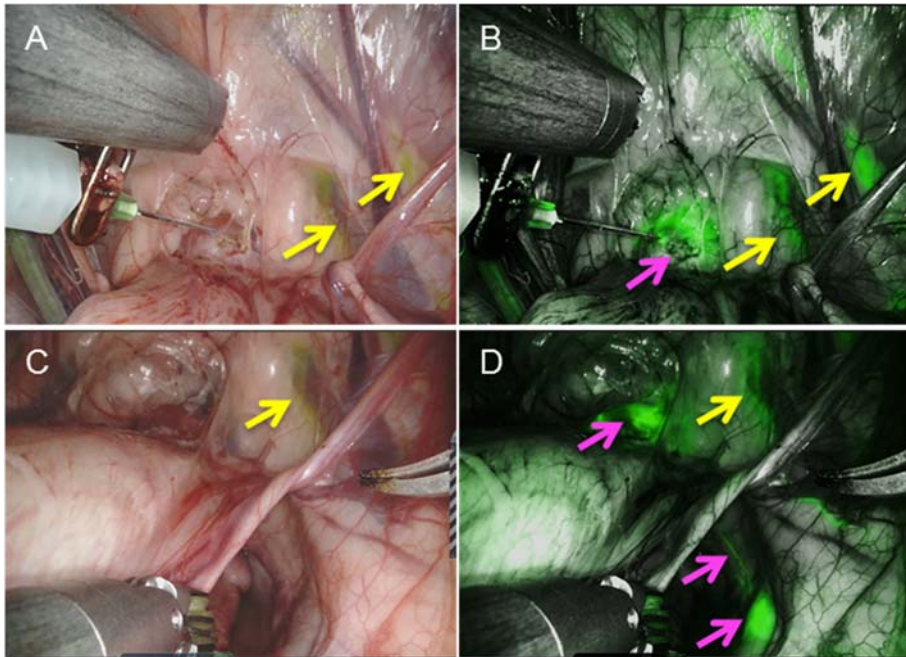


FIGURE 2. Multispectral-fluorescence imaging with the da Vinci Xi system. (A) Imaging during the intraprostatic administration of indocyanine green (ICG)-nanocolloid, depicting fluorescein in the white light image, (B) while the fluorescence image presents both fluorescein and ICG. (C) Imaging in white light following the lymphatic drainage of ICG-nanocolloid shows fluorescein positive areas (yellow arrow), (D) while fluorescence imaging clearly depicts an ICG-draining lymphatic duct and a sentinel node (pink arrows).

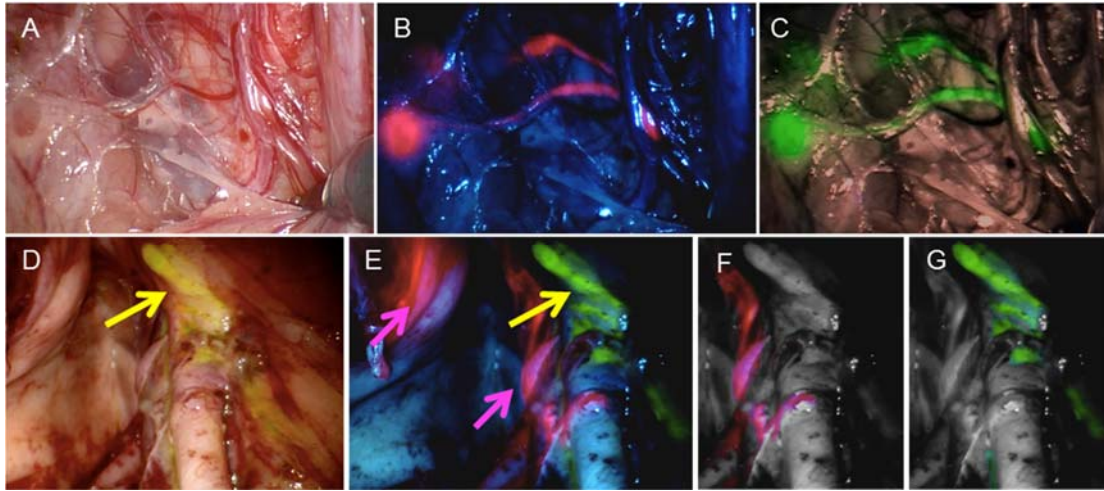


FIGURE 3. Multispectral-fluorescence imaging with the da Vinci Si system. Image series of lymphatic ducts and two sentinel nodes containing indocyanine green (ICG)-nanocolloid; (A) white light, (B) unprocessed image (ICG pink), (C) processed image (ICG green). Lymphatics in the external iliac region; (D) white light imaging displaying a fluorescein containing lymph duct (yellow arrow), (E) unprocessed multispectral-imaging simultaneously displays a SN (pink arrow) and the fluorescein stained lymph duct (yellow arrow), with the two signals digitally separated in (F) ICG and (G) fluorescein.

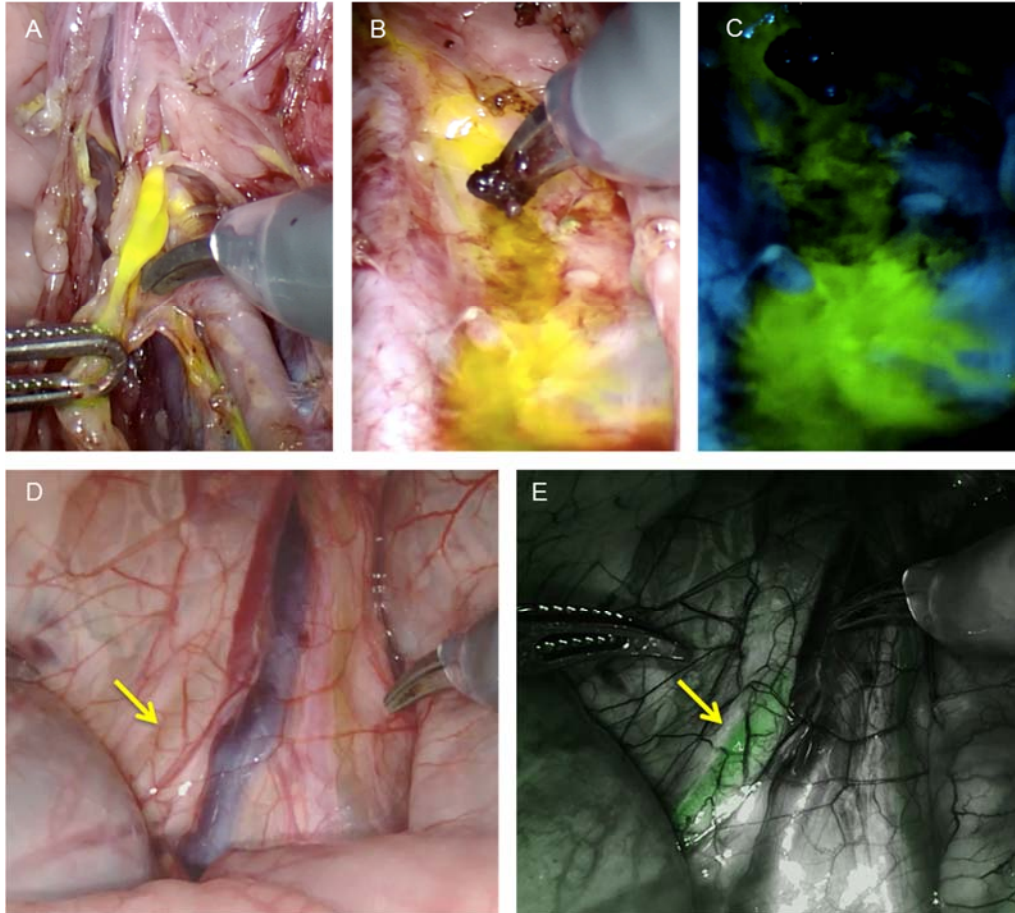


FIGURE 4. Additional values offered by fluorescein usage. (A) Surgical damage of a fluorescein containing lymph duct (Si-system). (B) As a consequence of the damage, the lymphatics leak fluorescein, staining the surgical field in white light and (C) fluorescence mode. (D) Depiction of a fluorescein containing ureter (yellow arrow; Xi-system) in white light and (E) fluorescence mode.

TABLE 1: Overview findings

Surgical system (# case)	Time between fluorescein injection and intraoperative imaging	Massage fluorescein injection site required for detection	Recording unprocessed images	Injection leg(s) fluorescein	Fluorescein visualization ureter	Fluorescein visualization lymphatic ducts	Number of LNs visualized using fluorescein	ICG-nanocolloid visualization lymphatic ducts	ICG-nanocolloid visualization SNs
Da Vinci Si									
2	150 min	yes	yes	R	Yes	yes	- LNs (L) 3 LNs (R)	yes	2 SNs (L) 1 SN (R)
3	80 min	N/A	yes	L+R	Not evaluated	yes	2 LNs (L) 3 LNs (R)	yes	1 SN (L) 1 SN (R)
4	92 min	N/A	yes	L+R	Not evaluated	yes	5 LNs (L) 4 LNs (R)	yes	1 SNs (L) 1 SNs (R)
Da Vinci Xi									
1	145 min	N/A	no	R	Yes	yes	- LNs (L) 5 LNs (R)	yes	2 SNs (L) 1 SN (R)
5	70 min	N/A	no	L+R	Yes	yes	4 LNs (L) 3 LNs (R)	yes	1 SN (L) 1 SNs (R)
Average	107 min						3.6 LNs/leg (L) 3.6 LNs/leg (R)		1.4 SNs (L) 1.0 SNs (R)



The Journal of
NUCLEAR MEDICINE

Multispectral fluorescence imaging as a tool to separate healthy and disease related lymphatic anatomies during robot-assisted laparoscopic procedures.

Philippa Meershoek, Gijs H KleinJan, Matthias N van Oosterom, Esther M Wit, Danny M van Willigen, Kevin P Bauwens, Erik J van Gennep, Alexandre M Mottrie, Henk G van der Poel and Fijs van Leeuwen

J Nucl Med.

Published online: May 18, 2018.

Doi: 10.2967/jnumed.118.211888

This article and updated information are available at:
<http://jnm.snmjournals.org/content/early/2018/05/17/jnumed.118.211888>

Information about reproducing figures, tables, or other portions of this article can be found online at:
<http://jnm.snmjournals.org/site/misc/permission.xhtml>

Information about subscriptions to JNM can be found at:
<http://jnm.snmjournals.org/site/subscriptions/online.xhtml>

JNM ahead of print articles have been peer reviewed and accepted for publication in *JNM*. They have not been copyedited, nor have they appeared in a print or online issue of the journal. Once the accepted manuscripts appear in the *JNM* ahead of print area, they will be prepared for print and online publication, which includes copyediting, typesetting, proofreading, and author review. This process may lead to differences between the accepted version of the manuscript and the final, published version.

The Journal of Nuclear Medicine is published monthly.
SNMMI | Society of Nuclear Medicine and Molecular Imaging
1850 Samuel Morse Drive, Reston, VA 20190.
(Print ISSN: 0161-5505, Online ISSN: 2159-662X)

© Copyright 2018 SNMMI; all rights reserved.

The logo for the Society of Nuclear Medicine and Molecular Imaging (SNMMI) features the letters 'S', 'N', 'M', and 'I' in a white, sans-serif font, each contained within a red square. The squares are arranged in a 2x2 grid.
SOCIETY OF
NUCLEAR MEDICINE
AND MOLECULAR IMAGING